Asian Journal of Chemistry; Vol. 38, No. 9 (2026), 2332-2340
ASIAN JOURNAL OF CHEMISTRY
https://doi.org/10.14233/ajchem.2026.36032

Design, Synthesis, Docking-Based Virtual Screening and Anticonvulsant Evaluation of Novel Isatin-linked Benzothiazole Hybrids

BHAVANA DUBEY[1], KULDEEP SINGH[1,*], ARUN KUMAR[1], SYED MISBAHUL HASAN[1], SUVAIV[1], SHOM PRAKASH KUSHWAHA[1] and PRAVEEN KUMAR[2]

[1]Department of Pharmacy, Faculty of Pharmacy, Integral University, Lucknow-226026, India
[2]Faculty of Pharmacy, Uttar Pradesh University of Medical Sciences, Saifai-206130, India

*Corresponding author: E-mail: kuldeep@iul.ac.in

Received: 17 March 2026 *Accepted*: 30 July 2026 *Published online*: 5 September 2026 AJC-22461

Benzothiazole and isatin scaffolds possess considerable biological importance and their molecular hybridization may provide a promising approach for enhancing anticonvulsant activity. The present study focused on the design, synthesis and evaluation of a novel series of 6-substituted-*N*′-(5-substituted-2-oxoindolin-3-ylidene)benzo[*d*]thiazole-2-carbohydrazide derivatives (**IBS01-IBS08**) using computational and experimental approaches. Molecular docking studies were performed using AutoDock 1.5.6 against γ-aminobutyric acid (GABA) aminotransferase (PDB ID: 1OHV) to investigate the binding interactions of the synthesized derivatives. The compounds were synthesized and characterized by IR, NMR and mass spectrometry. Their anticonvulsant activity was evaluated *in vivo* using the maximum electroshock seizure (MES) model at doses of 30 and 100 mg/kg, with hind-limb tonic extension (HLTE) used as the primary endpoint. Phenytoin (25 mg/kg, i.p.) served as the reference standard. The rotarod test was employed to assess motor coordination deficits. The docking results shows the valuable binding interactions of the synthesized hybrids with GABA-aminotransferase. All derivatives markedly decreased the duration of MES-induced HLTE without causing death. Phenytoin demonstrated significant anticonvulsant efficacy (***$p < 0.0001$) throughout all convulsive phases. The Rotarod test revealed no significant neurotoxic effects at the tested active doses. The synthesized benzothiazole-isatin hybrids exhibited significant anticonvulsant activity, favourable *in silico* binding affinity and low neurotoxicity, supporting their potential as lead structures for further development of antiepileptic agents.

Keywords: Benzothiazole derivatives, Isatin, Anticonvulsant activity, MES model, Molecular docking, GABA-aminotransferase.

INTRODUCTION

Nitrogen- and sulfur-containing heterocycles occupy an important position in medicinal chemistry due to their broad pharmacological profiles, including anticonvulsant activity [1]. Benzothiazole and isatin are two well-established scaffolds that have attracted interest in the development of CNS-active compounds owing to their diverse biological properties [2-4]. Combining these frameworks through molecular hybridization provides an opportunity to integrate their structural and pharmacological features within a single molecule. The molecular docking studies can further help the evaluation of ligand–target interactions and provide a basis for structural modification. The diverse biological responses reported for structurally modified benzothiazole derivatives support continued exploration of this scaffold for the development of new therapeutic candidates [5].

Anticonvulsant agents mainly act through modulation of ion channels, neurotransmitter systems and enzymes involved in neuronal excitability. Hybrid molecules combining more than one pharmacophore, such as isatin-benzothiazole derivatives, may interact with multiple biological targets and provide a broader pharmacological profile [6]. The clinical use of existing antiepileptic drugs is still limited by drug resistance and adverse effects, developing a need for new chemical scaffolds with improved efficacy and safety [7]. The biological activity of isatin is strongly influenced by its functional groups and the nature and position of substituents on its ring system [8].

Epilepsy is a chronic neurological disorder commonly treated with antiepileptic drugs, although drug resistance and adverse effects remain major challenges [9]. Molecular hybridization of benzothiazole and isatin offers a rational strategy for developing new anticonvulsant agents by combining the pharmacological features of both scaffolds within a single

framework [10,11]. The present study focused on the molecular hybridization of benzothiazole and isatin pharmacophores and examined the effect of shifting substitution from the 5- to the 6-position of the benzothiazole ring on anticonvulsant activity. This structural modification was based on the possibility that 6-substitution could provide a favourable arrangement for CNS activity. The selected derivatives were guided by reported structure activity relationships, with emphasis on the electronic and steric effects of the substituents [12]. The benzothiazole-isatin framework was selected to combine the pharmacological features of both scaffolds within a single molecular architecture and to explore their potential for developing new CNS-active anticonvulsant agents [13,14].

EXPERIMENTAL

All chemicals and reagents procured from Sigma-Aldrich, Shubh Scientific Corporation and InspiroChem were of analytical grade and used without further purification. Melting points were determined using an open-capillary melting point apparatus. Reaction progress was monitored by thin-layer chromatography (TLC) on silica gel 60 F_{254} plates (Merck), using hexane-ethyl acetate and chloroform-methanol as mobile phases. The developed TLC plates were examined under UV light. ^{1}H NMR spectra were recorded on JEOL and Bruker spectrometers using DMSO-d_6 as the solvent. FT-IR spectra were obtained using a Shimadzu FT-IR 8400S spectrophotometer using KBr pellets. Anticonvulsant activity was evaluated using the maximum electroshock seizure (MES) method.

Synthesis of ethyl 6-substituted-benzo[*d*]thiazole-2-carboxylate (DI-03A, 03B & 03C) (Step-1): A mixture of 2-amino-5-substituted-benzenethiol (1.0 g, 6.26 mmol) and diethyl oxalate (1.7 mL, 12.52 mmol) was heated at 140 ºC for 8 h, with the reaction progress monitored by TLC. After completion, the reaction mixture was cooled to room temperature and slowly added, with continuous stirring, to a mixture of HCl (5 mL), H_2O (15 mL) and C_2H_5OH (7 mL). The resulting solid was collected by vacuum filtration, washed with water and recrystallized from methanol to obtain the desired product [15].

Synthesis of 6-Substituted benzo[*d*]thiazole-2-carbohydrazide (DI-04A, 04B & 04C) (Step-2): Hydrazine (0.66 mL, 20.7 mmol) was added to an ethyl 6-substituted-benzo[*d*]-thiazole-2-carboxylate (1.0 g, 4.14 mmol) in ethanol (20 mL). The reaction mixture was stirred at room temperature for 2 h, and the progress was monitored by TLC. After completion, excess hydrazine was removed under high vacuum. The resulting residue was triturated with ethanol (10 mL) to afford the desired solid product [16].

Synthesis of titled compounds (IBS01-08) (Step-3): A catalytic amount of CH_3COOH was added to a stirred solution of ethyl 6-substituted-benzo[*d*]thiazole-2-carbohydrazide (0.5 g, 2.20 mmol) and 5-substituted-indoline-2,3-dione (0.6 g, 2.20 mmol) in ethanol (10 mL). The reaction mixture was heated with continuous stirring for 5 h, and the progress of the reaction was monitored by TLC. After completion, the mixture was cooled to room temperature and the resulting precipitate was collected by filtration and finally dried *in vacuo* (**Scheme-I**). The crude products were recrystallized from ethanol to afford the desired benzothiazole-isatin derivatives (**IBS01-IBS08**).

6-Chloro-*N*′-(5-iodo-2-oxoindolin-3-ylidene)benzo[*d*]-thiazole-2-carbohydrazide (IBS-01): Orange solid, yield: 0.67 g (63%); m.p.: 296-298 ºC, R_f: 0.35 (*n*-hexane:ethyl acetate 4:1); IR (KBr, ν_{max}, cm^{-1}): 3313, 3156 (NH *str.*), 3019 (C-H *str.*), 1715, 1689 (C=O), 1614 (C=C *str.*), 1580 (C=N *str.*), 1310, 1152, 915, 810, 724 (C-Cl); ^{1}H NMR (400 MHz, DMSO-d_6, δ ppm): 14.32 (s, 1H, NH), 11.56 (s, 1H, -NH isatin), 8.45 (s, 1H, ArH), 8.20 (d, 1H, ArH), 7.83 (s, 1H, ArH), 7.73-7.69 (m, 2H, ArH), 6.82 (d, 1H, ArH); MS: (*m/z*) 483.3 $(M)^+$, 485.5 $(M+2)^+$.

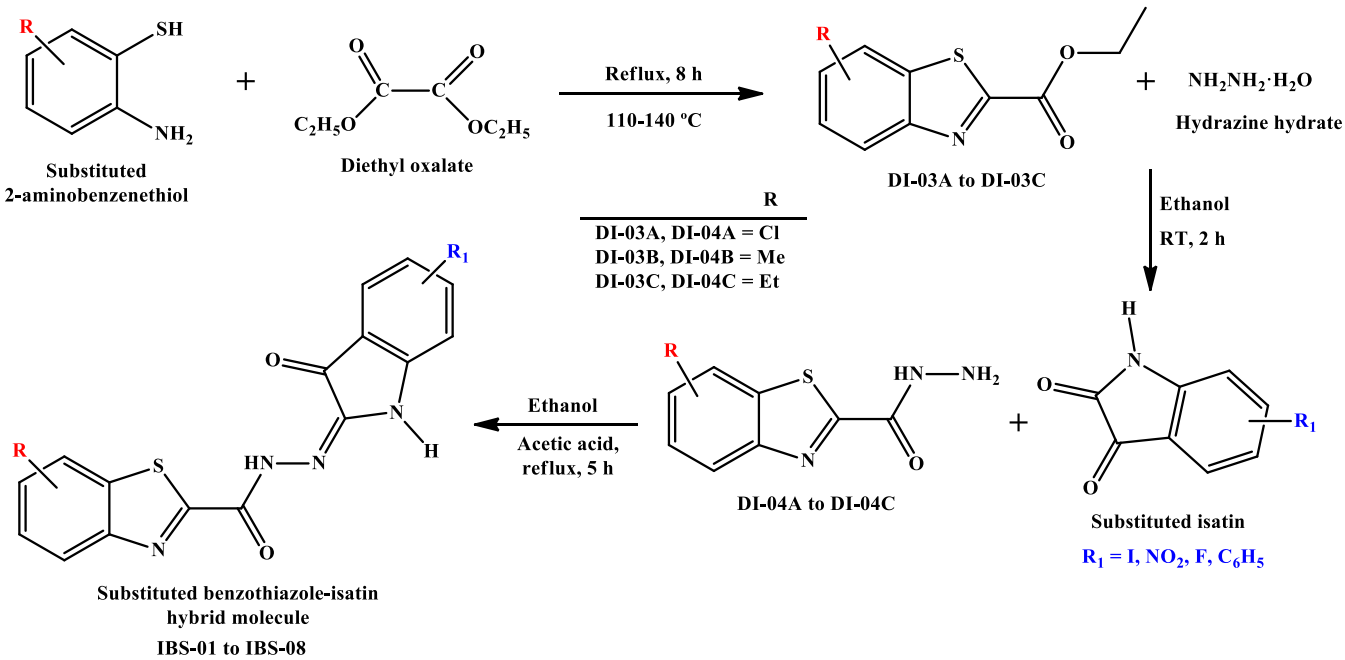

Scheme-I: Synthesis of 6-substituted-*N*′-(5-substituted-2-oxoindolin-3-ylidene)benzo[*d*]thiazole-2-carbohydrazide derivatives (**IBS-01–08**)

6-Chloro-*N′*-(5-nitro-2-oxoindolin-3-ylidene)benzo[*d*]-thiazole-2-carbohydrazide (IBS-02): Yellow solid, yield: 0.52 g (59%); m.p.: 294-296 ºC, R_f: 0.312 (*n*-hexane:ethyl acetate 4:1); IR (KBr, ν_{max}, cm^{-1}): 3234, 3180 (NH *str.*), 3010, 2936 (C-H *str.*), 1719, 1678 (C=O), 1628 (C=C *str.*), 1529 (C=N *str.*), 1513 and 1343 (N=O *str.*), 1143, 914, 854, 764 (C-Cl); ^{1}H NMR (400 MHz, DMSO-d_6, δ ppm): 14.17 (s, 1H, NH), 11.96 (s, 1H, -NH isatin), 8.42 (d, 1H, ArH), 8.31-8.28 (m, 1H, ArH), 8.24 (s, 1H, ArH), 8.18 (d, 1H, ArH), 7.70-7.67 (m, 1H, ArH), 7.14-7.11 (m, 1H, ArH); MS (*m/z*): 400.3 $(M-1)^+$.

6-Chloro-*N′*-(5-fluoro-2-oxoindolin-3-ylidene)benzo[*d*]-thiazole-2-carbohydrazide (IBS-03): Yellow solid, yield: 0.73 g (72%); m.p.: 222-224 ºC, R_f: 0.33 (*n*-hexane:ethylacetate 4:1); IR (KBr, ν_{max}, cm^{-1}): 3261, 3137 (NH *str.*), 3010 (C-H *str.*), 1709, 1670 (C=O), 1595 (C=C *str.*), 1520 (C=N *str.*), 1479, 1166, 914, 814, 724 (C-Cl); ^{1}H NMR (400 MHz, DMSO-d_6, δ ppm): 11.399 (s, 1H, NH), 11.011 (s, 1H, -NH isatin), 7.749-7.433 (m, 4H, ArH), 7.427-7.226 (m, 1H, ArH), 6.984-6.903 (m, 1H, ArH); MS: (*m/z*) 375.13 $(M)^+$, 377.14 $(M+2)^+$.

***N′*-(5-Iodo-2-oxoindolin-3-ylidene)-6-methylbenzo[*d*]-thiazole-2-carbohydrazide (IBS-04):** Orange solid, yield: 0.70 g (63%); m.p.: 296-298 ºC, R_f: 0.62 (*n*-hexane:ethyl acetate 4:1); IR (KBr, ν_{max}, cm^{-1}): 3281, 3173 (NH *str.*), 3069, 2921 (C-H *str.*), 1703, 1691 (C=O), 1580 (C=C *str.*), 1513 (C=N *str.*), 1493, 1147, 917, 810, 714, 579; ^{1}H NMR (400 MHz, DMSO-d_6, δ ppm): 14.33 (s, 1H, -NH), 11.47 (s, 1H, -NH isatin), 8.12-8.08 (m, 2H, ArH), 7.86 (s, 1H, ArH), 7.75-7.73 (m, 1H, ArH), 7.53-7.51 (m, 1H, ArH), 6.83-6.81 (m, 1H, ArH), 2.51 (s, -CH_3); MS: *m/z* 461.4 $(M-1)^+$.

6-Methyl-*N′*-(5-nitro-2-oxoindolin-3-ylidene)benzo[*d*]-thiazole-2-carbohydrazide (IBS-05): Yellow solid, yield: 0.56 g (61%); m.p.: 244-246 ºC, R_f: 0.38 (*n*-hexane:ethyl acetate 4:1); IR (KBr, ν_{max}, cm^{-1}): 3226, 3120 (NH *str.*), 3050, 2921 (C-H *str.*), 1717, 1677 (C=O), 1626 (C=C *str.*), 1532 (C=N *str.*), 1530, 1342 (N=O *str.*), 1142, 919, 817, 693; ^{1}H NMR (400 MHz, DMSO-d_6, δ ppm): 14.24 (s, 1H, -NH), 11.99 (s, 1H, -NH isatin), 8.34-8.31 (m, 2H, ArH), 8.13-8.10 (m, 2H, ArH), 7.59-7.57 (m, 1H, ArH), 7.18-7.16 (d, 1H, ArH), 2.51 (s, -CH_3); MS: (*m/z*) 380.5 $(M-1)^+$.

***N′*-(5-Fluoro-2-oxoindolin-3-ylidene)-6-methylbenzo-[*d*]thiazole-2-carbohydrazide (IBS-06):** Yellow solid, yield: 0.60 g (71%); m.p.: 222-224 ºC R_f: 0.57 (*n*-hexane:ethylacetate 4:1); IR (KBr, ν_{max}, cm^{-1}): 3299, 3156 (NH *str.*), 3054, 2922 (C-H *str.*), 1719, 1687 (C=O), 1626 (C=C *str.*), 1518 (C=N *str.*), 1480, 1141, 917, 823, 722, 578. ^{1}H NMR (400 MHz, DMSO-d_6, δ ppm): 14.40 (s, 1H, -NH), 11.37 (s, 1H, -NH isatin), 8.12-8.08 (m, 2H, ArH), 7.53-7.46 (m, 2H, ArH), 7.29-7.25 (m, 1H, ArH), 6.98-6.95 (m, 1H, ArH), 2.51 (s, -CH_3); MS: *m/z* 355.1 $(M+1)^+$.

6-Methyl-*N′*-(2-oxo-5-phenylindolin-3-ylidene)benzo-[*d*]thiazole-2-carbohydrazide (IBS-07): Orange solid, yield: 0.67 g (68%); m.p.: 295-297 ºC R_f: 0.71 (*n*-hexane:ethyl acetate 4:1); IR (KBr, ν_{max}, cm^{-1}): 3464, 3346 (NH *str.*), 3061, 3026, 2913 (C-H *str.*), 1732, 1698 (C=O), 1624 (C=C *str.*), 1514 (C=N *str.*), 1477, 1144, 917, 814, 754, 697; ^{1}H NMR (400 MHz, DMSO-d_6, δ ppm): 14.43 (s, 1H, -NH), 11.03 (s, 1H, -NH isatin), 8.31 (s, 1H, ArH), 8.12-8.09 (m, 2H, ArH), 8.01 (d, 1H, ArH), 7.85-7.79 (m, 3H, ArH), 7.60-7.44 (m, 3H, ArH), 7.06 (d, 1H, ArH), 2.51 (s, -CH_3); MS: *m/z* 413.4 $(M+1)^+$.

6-Ethyl-*N′*-(5-iodo-2-oxoindolin-3-ylidene)benzo[*d*]-thiazole-2-carbohydrazide (IBS-08): Orange solid, yield: 0.71 g (66%); m.p.: 297-299 ºC R_f: 0.63 (*n*-hexane:ethyl acetate 4:1); IR (KBr, ν_{max}, cm^{-1}): 3381, 3151 (NH *str.*), 3061, 2969 (C-H *str.*), 1708, 1689 (C=O), 1614 (C=C *str.*), 1513 (C=N *str.*), 1484, 1152, 915, 854, 725, 672; ^{1}H NMR (400 MHz, DMSO-d_6, δ ppm): 14.34 (s, 1H, -NH), 11.46 (s, 1H, -NH isatin), 8.14-8.12 (m, 2H, ArH), 7.88-7.86 (m, 1H, ArH), 7.75-7.73 (m, 1H, ArH), 7.55 (d, 1H, ArH), 6.81 (d, 1H, ArH), 2.81 (q, 2H, J = 7.6 Hz, -CH_2CH_3), 1.28 (t, 3H, J = 7.6 Hz, -CH_2CH_3); MS: *m/z* 475.3 $(M-1)^+$.

Molecular docking: The crystal structure of 4-amino-butyrate-aminotransferase sourced from pig (PDB ID: 1OHV) acquired from the RCSB protein data library, facilitating a molecular docking study [17]. The protein structures were pre-processed by modelling missing loops, adding absent atoms, removing alternate conformations, standardizing atom nomenclature, and assigning appropriate protonation states to titratable residues. Crystallographic water molecules were removed, followed by energy minimization of the prepared structures prior to molecular docking [18].

The ligands were drawn using ChemDraw and saved in CDX format. Their geometries were optimized using Chem3D 15.0, followed by conversion to SDF format. ChemDraw Professional 15.0 was used to generate the corresponding PDB files. Ligand preparation for docking was carried out using AutoDockTools 1.5.6. Torsional flexibility was defined by assigning rotatable bonds, while the remaining bonds were kept fixed. The prepared ligands were saved in PDBQT format for docking calculations.

Molecular docking simulations were performed using BIOVIA Discovery Studio 2022 Client. The binding pocket of each receptor was selected as the active site, with consideration of both polar and nonpolar regions to facilitate appropriate ligand placement [19]. Protein–ligand interactions were assessed based on docking scores and two-dimensional interaction images.

Anticonvulsant screening: The present study was carried out in Department of Pharmacology, Animal House, Integral University, Lucknow, following approval from the Institutional Animal Ethics Committee (IU/IAEC/10/02/2025). Seizures were induced in Swiss albino mice using the maximal electroshock (MES) method [20]. The experimental setup included polypropylene cages, a Medicraft electroconvulsiometer, a timer, gavage feeding tubes, phenytoin sodium, ear-clip electrodes and Swiss albino mice.

Healthy Swiss albino mice weighing 20-30 g and aged 8-12 weeks were selected for the study. Before experimentation, the animals were acclimatized for 1 week under controlled laboratory conditions. The animals were maintained under a 12 h light/12 h dark cycle at a controlled temperature, with free access to standard pellet feed and water. All experimental procedures were performed during the light phase. The study was conducted in accordance with the guidelines and protocols approved by the Institutional Animal Ethics Committee (IAEC).

Grouping and dosing of animals: The antiepileptic potential of compounds **IBS01-IBS08** was evaluated using an *in vivo* MES-induced seizure model. Ten groups of Swiss albino mice (n = 5 per group) were randomly assigned for the experiment. The control group received MES stimulation without test treatment, while phenytoin (25 mg/kg, i.p.) was administered as the standard anticonvulsant to validate the experimental model [21].

The remaining eight groups received the respective test compounds at doses of 30 and 100 mg/kg, administered intraperitoneally. Following MES induction, the animals exhibited distinct seizure phases, including tonic flexion, tonic extension, clonic convulsions, stupor and subsequent recovery or mortality. Hind limb tonic extension (HLTE) was defined as a sustained extension of the hind limbs at an angle higher than 90º from the body axis for more than 3 s [22]. The duration of the HLTE phase was recorded for each treatment group as a measure of seizure severity. A reduction or complete absence of HLTE was considered indicative of anticonvulsant protection. In the MES model, HLTE serves as the primary endpoint and provides a measure of susceptibility to electrically induced seizure activity [23].

Maximal electroshock-Induced seizures (MES) test: The anticonvulsant activity of the synthesized compounds was evaluated using the maximal electroshock (MES) method. Seizures were induced in mice using an electroconvulsiometer by applying a 50 mA current for 0.2 s through ear-clip electrodes. MES stimulation elicited characteristic tonic seizures, marked by sustained extension of the forelimbs and hind limbs. Tonic hind limb extension (THLE) was considered the principal endpoint for assessing seizure severity. The tonic phase was followed by clonic convulsions, characterized by limb paddling and body tremors. A reduction or complete absence of THLE was considered evidence of protection against MES-induced seizures. Following the seizure episode, the animals gradually returned to their normal posture and locomotor activity. Seizure responses were monitored and video-recorded for 2-3 min to facilitate accurate assessment. The synthesized compounds exhibited appreciable anticonvulsant activity, as indicated by a reduction in THLE duration compared with the control group [24].

Swiss albino mice of either sex, weighing 25-30 g, were randomly divided into ten groups, with five animals in each group (n = 5). The animals were fasted overnight before the experiment, with access to water maintained during the fasting period. Prior to the experimental assessment, food and water were withheld as per the study protocol. The test compounds (**IBS01**-**IBS08**) were dissolved in propylene glycol and administered intraperitoneally at doses of 30 and 100 mg/kg. The control group received the vehicle, while the standard group was treated with phenytoin (25 mg/kg, i.p.). The remaining eight groups received the respective test compounds. Seizure activity was assessed at 30 min after treatment. The temperature was maintained under controlled conditions throughout the experiment, as temperature fluctuations can influence seizure susceptibility. Lower temperatures may reduce the seizure threshold, whereas higher temperatures may increase the likelihood of seizure activity [25].

Statistical analysis: The data were analyzed using GraphPad Prism software, version 10.6.1 (892; GraphPad Software, Inc.). Statistical comparisons were performed using one-way analysis of variance (ANOVA), followed by Dunnett's multiple comparison test.

RESULTS AND DISCUSSION

A three-step synthetic route (**Scheme-I**) was applied to synthesize compounds **IBS01-IBS08**. In the first step, 2-amino-5-substituted-benzenethiol (1.0 g, 6.26 mmol) was reacted with diethyl oxalate (1.7 mL, 12.52 mmol) at 140 ºC for 8 h. After completion, the reaction mixture was added to a mixture of HCl (5 mL), H_2O (15 mL) and ethanol (7 mL). The resulting solid was filtered, washed with water and recrystallized from methanol to obtain ethyl 6-substituted benzo[*d*]-thiazole-2-carboxylates (**DI-03A-C**). These intermediates (1.0 g, 4.14 mmol) were treated with hydrazine hydrate (0.66 mL, 20.7 mmol) in ethanol (20 mL) for 2 h. Th excess hydrazine was removed under reduced pressure and the residue was triturated with ethanol to afford the corresponding carbohydrazides (**DI-04A-C**). In the final step, carbohydrazides (0.5 g, 2.20 mmol) were condensed with 5-substituted-indoline-2,3-diones (0.6 g, 2.20 mmol) in ethanol (10 mL) in the presence of a few drops of acetic acid. The reaction mixture was heated for 5 h, with progress monitored by TLC. The precipitated products were filtered, washed and recrystallized from ethanol to obtain **IBS01-IBS08**. The synthesized compounds were obtained as crystalline solids in 61-75% yields and their melting points were determined.

The synthesized derivatives were characterized by FT-IR and ^{1}H NMR spectroscopy. The FT-IR spectra showed characteristic bands at 3465-3120 cm^{-1} corresponding to N–H stretching, 3070-2912 cm^{-1} for C–H stretching, 1732-1670 cm^{-1} for C=O stretching and 1626-1580 cm^{-1} for C=C stretching. Bands assigned to C=N and N=O stretching appeared at 1580-1512 and 1530-1342 cm^{-1}, respectively, while the bands in the 1494-557 cm^{-1} region were associated with C–Cl/C–Br vibrations. The ^{1}H NMR spectra of **IBS01-IBS08** displayed downfield singlets at δ 14.33-14.17 and 12.29-12.22 ppm attributable to NH protons, along with a signal at δ 11.96-11.19 ppm assigned to the isatin NH proton. Aromatic protons appeared mainly in the δ 8.48-7.25 ppm region, with signals around δ 8.20-8.18 ppm assigned to benzothiazole protons. For the 6-methyl-substituted derivatives, the methyl protons appeared as a singlet at δ 2.51-2.49 ppm. The ethyl substituted derivatives exhibited signals in the δ 2.85-1.26 ppm region corresponding to the CH_2CH_3 group.

Molecular docking studies: Molecular docking studies of the synthesized compounds were performed using AutoDock 1.5.6, with BIOVIA Discovery Studio 2022 used for visualization and analysis of the ligand–protein interactions. Porcine 4-aminobutyrate aminotransferase (GABA-AT; PDB ID: 1OHV) was selected as the target to examine the binding potential of the synthesized derivatives in relation to their anticonvulsant activity. The calculated docking scores ranged from -0.52 to -9.75 kcal/mol, with several derivatives showing favourable binding compared with the reference drug carbamazepine (-7.17 kcal/mol).

Among the synthesized compounds, **IBS02**, **IBS05** and **IBS04** showed the most favourable docking scores of -9.75, -9.61 and -8.92 kcal/mol, respectively. These compounds formed three to four hydrogen bonds with key active-site residues including Phe189, Val300 and Ile72 (Fig. 1). IBS03 showed a docking score of -4.32 kcal/mol, whereas IBS01 exhibited the lowest score (-0.52 kcal/mol). Other derivatives interacted with residues such as Cys135, Thr353, Ser137, Asn352, Arg192, His190 and Gly135 through hydrogen bonding and other non-covalent contacts. The docking scores and interaction profiles are shown in Table-1.

The binding analysis showed that besides hydrogen bonds, the derivatives formed π-alkyl, π-anion, π-π stacking, π-π T-shaped and van der Waals interactions within the active site. Derivatives carrying electron-withdrawing groups exhibited more favourable docking scores, while the substituent position and electronic character influenced their interactions within the enzyme pocket. **IBS02** recorded the best docking score among the tested derivatives and formed multiple interactions with key residues of the active site. Fig. 1 shows 2D and 3D representations of the synthesized compounds (**IBS01-IBS08**) and the reference drug, carbamazepine.

GABA-aminotransferase is a pyridoxal-5′-phosphate dependent mitochondrial enzyme involved in GABA catabolism. It converts GABA to succinic semialdehyde, which is subsequently metabolized to succinate through the GABA shunt. Inhibition of GABA-AT reduces GABA degradation and can increase the availability of GABA for activation of $GABA_A$ and $GABA_B$ receptors, strengthening inhibitory neurotransmission.

The docking results indicate that the benzothiazole-isatin hybrids can adopt favourable orientations within the GABA-AT binding pocket. The combination of hydrogen bonding, hydrophobic contacts, π-interactions and van der Waals forces

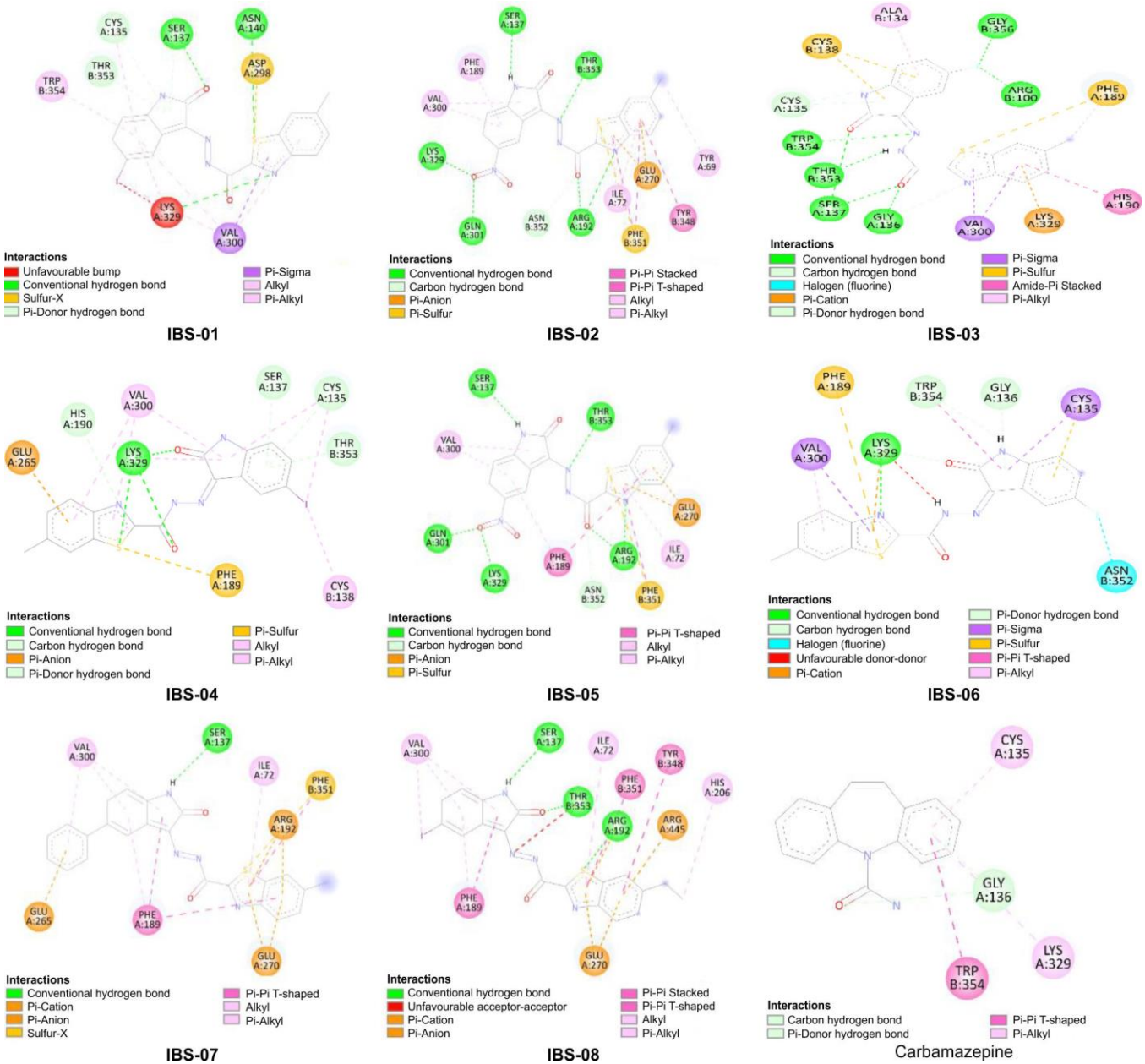

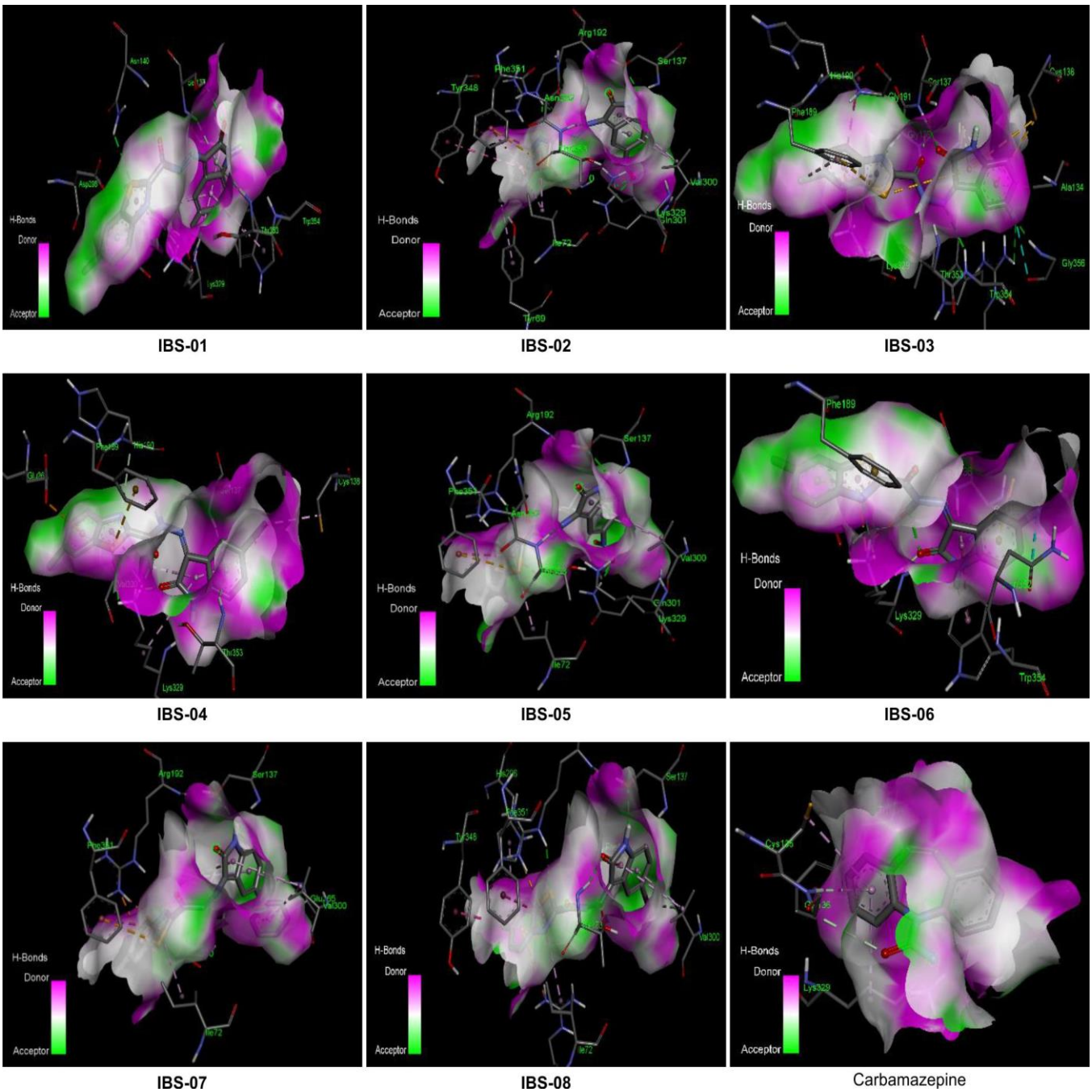

Fig. 1. Two-dimensional and three-dimensional schematic representations of the synthesized compounds (**IBS-01–08**) and reference drug carbamazepine

TABLE-1
DOCKING SCORES (kcal/mol) OF SYNTHESIZED COMPOUNDS (**IBS-01–08)** ASSOCIATED WITH PDB ID (1OHV)

Ligand	Receptor	Binding affinity	Interaction residues
Carbamazepine	$GABA_{AT}$	-7.17	Cys135, Trp354, Lys329
IBS-01	$GABA_{AT}$	-0.52	Trp354, Asp298, Lys329, Val300
IBS-02	$GABA_{AT}$	-9.75	Phe189, Val300, Ile72, Glu270, Phe351, Tyr348, Tyr69
IBS-03	$GABA_{AT}$	-4.32	Cys138, Ala134, Phe189, His190, Lys329
IBS-04	$GABA_{AT}$	-8.92	Glu265, Val300, Phe189, Cys138
IBS-05	$GABA_{AT}$	-9.61	Val300, Phe189, Ile72, Glu135, Asn352
IBS-06	$GABA_{AT}$	-8.89	Phe189, Val300, Cys135, Asn352
IBS-07	$GABA_{AT}$	-8.17	Val300, Ile72, Phe351, Arg192, Glu270, Phe189, Glu265
IBS-08	$GABA_{AT}$	-7.74	Val300, Phe189, Glu720, Arg445, Phe351, Ile72, Tyr348, His206

may contribute to their binding stability. These findings provide a basis for considering the synthesized derivatives, particularly **IBS02**, as potential GABA-AT-targeting anticonvulsant candidates. Since docking data alone cannot establish enzyme inhibition, biochemical studies are required to confirm their inhibitory activity and clarify the mechanism responsible for the observed anticonvulsant effects.

Anticonvulsant activity: The maximal electroshock (MES)-induced seizure model revealed a dose-dependent reduction in the duration of different convulsive phases following treatment with the synthesized hybrids derivatives compared with the disease control group. Animals in the disease control group exhibited prolonged seizure durations during the flexion (5.62 ± 0.31 s), extension (11.24 ± 0.41 s), clonus (6.28 ± 0.37 s) and stupor (12.41 ± 0.50 s) phases. Treatment with the standard drug significantly reduced the duration of all convulsive phases, confirming its anticonvulsant activity (Table-2).

Among the tested compounds, **IBS02** exhibited the strongest anticonvulsant activity, with marked reductions in the extension and stupor phases at doses of 30 and 100 mg/kg. At these doses, its activity was comparable to that observed in the standard control group. **IBS05** displayed the next highest protective effect, followed by **IBS04**, **IBS06**, **IBS07**, **IBS08**, **IBS03** and **IBS01** in decreasing order of efficacy. A significant reduction in tonic hind limb extension (HLTE) duration was recorded for **IBS02** at 100 mg/kg (**$p < 0.0001$), with seizure duration markedly reduced compared with the control group. All treated animals recovered during the observation period, and no mortality was recorded at the tested doses. The results were expressed as mean ± SEM and differences were considered statistically significant at $p < 0.05$. The statistical values in Figs. 2 and 3 were $p < 0.023$, $p < 0.0001$ and $p < 0.0001$; $p = 0.084$ was considered non-significant.

Motor coordination impairment (rotarod): Motor coordination impairment was evaluated using the rotarod test.

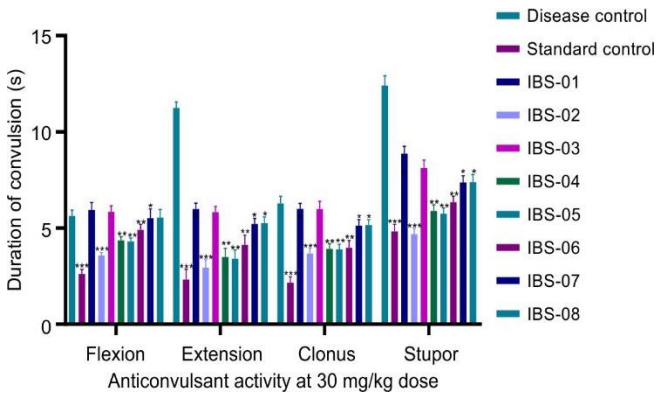

Fig. 2. Duration of different convulsive phases in the MES model at 30 mg/kg. Data are expressed as mean ± SEM (n = 5) and were analyzed by one-way ANOVA followed by Dunnett's multiple-comparison test. Significance levels were $p < 0.046$, *$p < 0.001$, and **$p < 0.0001$; $p = 0.16$ and 0.25 were non-significant

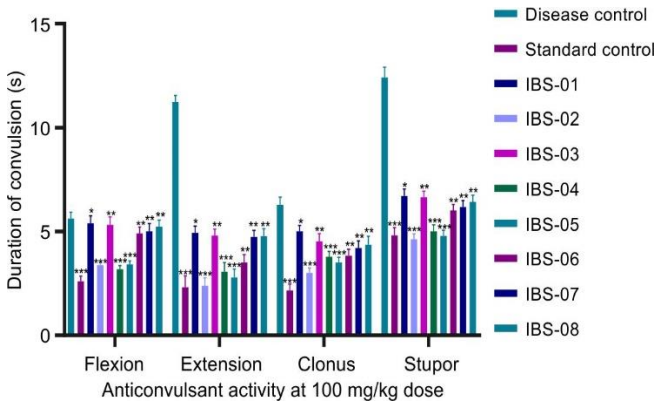

Fig. 3. Duration of different convulsive phases in the MES model at 100 mg/kg. Data are expressed as mean ± SEM (n = 5) and were analyzed by one-way ANOVA followed by Dunnett's multiple-comparison test. Significance levels were $p < 0.01$, *$p < 0.001$, and **$p < 0.0001$

TABLE-2
ANTICONVULSANT ACTIVITY DATA OF THE TEST GROUP (**IBS-01–08**)
AGAINST MAXIMAL ELECTROSHOCK (MES)-INDUCED SEIZURES IN MICE

Treatment	Dose	Different stages of seizure activity (time, s)				Recovery/death
		Flexion	Extension	Clonus	Stupor	
Disease control	0	5.62 ± 0.31	11.24 ± 0.41	6.28 ± 0.37	12.41 ± 0.50	Recovery
Standard control	25	2.61 ± 0.24	2.32 ± 0.54	2.16 ± 0.31	4.82 ± 0.37	Recovery
IBS-01	30	5.94 ± 0.38	5.98 ± 0.31	5.99 ± 0.29	8.87 ± 0.38	Recovery
	100	5.39 ± 0.37	4.94 ± 0.32	5.01 ± 0.28	6.71 ± 0.34	Recovery
IBS-02	30	3.56 ± 0.17	2.94 ± 0.41	3.67 ± 0.28	4.69 ± 0.29	Recovery
	100	3.38 ± 0.15	2.39 ± 0.38	3.01 ± 0.24	4.63 ± 0.26	Recovery
IBS-03	30	5.84 ± 0.31	5.83 ± 0.29	5.98 ± 0.41	8.12 ± 0.41	Recovery
	100	5.32 ± 0.38	4.81 ± 0.31	4.53 ± 0.37	6.65 ± 0.29	Recovery
IBS-04	30	4.36 ± 0.19	3.49 ± 0.46	3.91 ± 0.28	5.89 ± 0.32	Recovery
	100	3.18 ± 0.18	3.06 ± 0.44	3.78 ± 0.26	5.01 ± 0.31	Recovery
IBS-05	30	4.30 ± 0.18	3.41 ± 0.44	3.89 ± 0.27	5.74 ± 0.31	Recovery
	100	3.42 ± 0.17	2.79 ± 0.40	3.51 ± 0.25	4.78 ± 0.28	Recovery
IBS-06	30	4.91 ± 0.28	4.12 ± 0.51	3.98 ± 0.37	6.34 ± 0.35	Recovery
	100	4.90 ± 0.31	3.52 ± 0.37	3.84 ± 0.31	6.01 ± 0.29	Recovery
IBS-07	30	5.51 ± 0.48	5.21 ± 0.29	5.13 ± 0.30	7.37 ± 0.35	Recovery
	100	5.01 ± 0.37	4.74 ± 0.31	4.21 ± 0.34	6.18 ± 0.31	Recovery
IBS-08	30	5.54 ± 0.42	5.26 ± 0.31	5.15 ± 0.28	7.39 ± 0.39	Recovery
	100	5.24 ± 0.31	4.77 ± 0.37	4.36 ± 0.41	6.43 ± 0.32	Recovery

The mice were initially trained to maintain their balance on a rotating rod (3.2 cm in diameter) over three sessions, each lasting 60 s. During the training period, the animals remained on the rotating rod for 3 min to become accustomed to the continuous movement. Before the test, the mice received intraperitoneal administration of the respective test compounds. Motor performance was assessed at screening doses of 30 and 100 mg/kg before the MES study using the rotarod apparatus. Failure to remain on the rod for at least 1 min in all three trials was considered indicative of motor dysfunction [26].

In the neurotoxicity assessment, **IBS02**, **IBS04** and **IBS05** did not exhibit detectable neurotoxic effects even at 100 mg/kg. No appreciable impairment of motor coordination was observed with these compounds at either dose during the two observation periods. The remaining compounds exhibited signs of neurotoxicity at 100 mg/kg. Most of the synthesized derivatives caused less motor impairment than phenytoin under the same experimental conditions (Table-3).

TABLE-3
ASSESSMENT OF MOTOR COORDINATION IMPAIRMENT INDUCED BY COMPOUNDS IBS01-IBS08 USING THE ROTAROD TEST AT 0.5 AND 4 h FOLLOWING INTRAPERITONEAL ADMINISTRATION*

Motor coordination impairment (rotarod)		
Group	0.5 h	4.0 h
Standard control	100	100
IBS-01	100	100
IBS-02	–	–
IBS-03	100	100
IBS-04	–	–
IBS-05	–	–
IBS-06	–	100
IBS-07	–	100
IBS-08	–	100

Number of animals used: 5, Dose of 30 & 100 mg/kg were administered i.p. & The animals were examined at 0.5 h and 4 h after injections were administered. The dash (–) indicates an absence of activity at 100mg/kg dose administered.

Structure–activity relationship (SAR): Dimmock *et al.* [27] proposed a pharmacophore model for anticonvulsants that consist of (i) a hydrophobic domain, (ii) a hydrogen bonding domain (HBD), (iii) a distal hydrophobic domain and (iv) an electron donor moiety. Based on above proposal the compounds were synthesized (Fig. 4). Electron-withdrawing substituents enhance ligand binding within the GABA-AT active site by modulating the electronic distribution of the scaffold, thereby strengthening hydrogen-bonding and electrostatic interactions. Halogen substituents further contribute through hydrophobic contacts and possible halogen bonding with active site residues, leading to improved ligand stabilization [28,29]. Structure–activity relationship studies revealed that substitution at both R and R_1 positions markedly influenced the anticonvulsant activity of the synthesized benzothiazole–isatin hybrids. Electron-withdrawing substituents at the R position, particularly chloro, significantly enhanced activity, likely due to increased lipophilicity and favourable electronic effects, whereas alkyl substituents such as methyl group in benzothiazole ring is more active than ethyl group. Substitution at the R_1 position further modulated biological response, where the presence of a nitro group (–NO_2) exhibited potency for MES activity, while halogenated derivatives (Br, I and F) exhibited improved anticonvulsant activity but bulky aromatic substitution (–C_6H_5) led to diminished efficacy, possibly due to steric hindrance affecting receptor binding. Compounds bearing electron-withdrawing and moderately lipophilic substituents at the R and R_1 positions exhibited greater anticonvulsant activity. This trend suggests that electronic properties and an appropriate steric balance at these positions play an important role in enhancing anticonvulsant efficacy.

Conclusion

A novel series of 6-substituted-N′-(5-substituted-2-oxoindolin-3-ylidene)benzo[*d*]thiazole-2-carbohydrazide derivatives was successfully designed, synthesized and characterized. The spectral data are in agreement with the proposed structures and confirmed the purity of the synthesized derivatives.

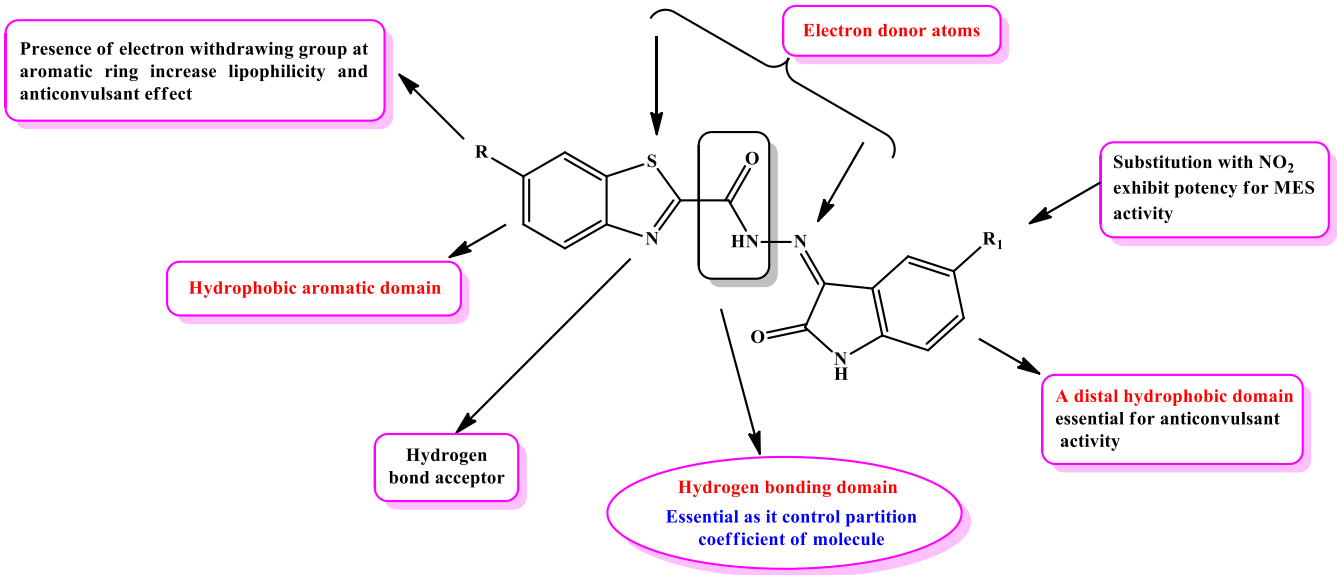

Fig. 4. Structure-activity relationship of synthesized compounds (where R = -Cl, -Me, -Et; R_1 = -I, -NO_2, -F, -C_6H_5)

Docking studies supported their ability to interact with epilepsy related protein targets, while pharmacological evaluation using the MES model established their anticonvulsant potential. **IBS02** and **IBS05** emerged as the most active compounds, providing substantial protection at 30 and 100 mg/kg. Neither **IBS02** nor **IBS05** caused significant impairment of motor coordination in the rotarod test at the evaluated doses. The combined pharmacological and molecular docking findings identify benzothiazole-isatin hybrids as promising scaffolds for further development of antiepileptic agents.

ACKNOWLEDGEMENTS

The authors thank the Faculty of Pharmacy, Integral University, Lucknow, India, for providing the necessary research laboratory infrastructure and animal housing facilities. The study was conducted in accordance with institutional and national ethical guidelines and the required ethical approval was obtained. The authors further acknowledge the Research Committee, Integral University, for providing the manuscript communication no. IU/R&D/2025-MCN0004166.

CONFLICT OF INTEREST

The authors declare that there is no conflict of interests regarding the publication of this article.

DECLARATION OF AI-ASSISTED TECHNOLOGIES

During the preparation of this manuscript, the authors used an AI-assisted tool(s) to improve the language and no data, results or scientific conclusions were generated by AI. All analyses, interpretations and conclusions are the authors' own. The authors reviewed and edited the content and take full responsibility for the published work.

REFERENCES

1. P. Singh, K. Nisa, R. Mavi, S. Yadav and R. Kumar, *Chem. Biodiver.*, **22**, e202401620 (2025); https://doi.org/10.1002/cbdv.202401620
2. S.S. Sulthana and P. Pandian, *J. Drug Deliv. Ther.*, **9(1S)**, 505 (2019); https://doi.org/10.22270/jddt.v9i1-s.2358
3. R.A. Mohamed-Ezzat and G.H. Elgemeie, *RSC Adv.*, **15**, 41724 (2025); https://doi.org/10.1039/D5RA03993B
4. J. Gagoria, P.K. Verma and A. Khatkar, *Cent. Nerv. Syst. Agents Med. Chem.*, **15**, 11 (2015); https://doi.org/10.2174/1871524915666150112094206
5. S. Kumar and B. Dubey, *J. Drug Deliv. Ther.*, **12(4S)**, 270 (2022); https://doi.org/10.22270/jddt.v12i4-S.5549
6. P.S. Auti, G. George and A.T. Paul, *RSC Adv.*, **10**, 41353 (2020); https://doi.org/10.1039/D0RA06642G
7. A. Kumar, A.K. Singh, H. Singh, V. Vijayan, D. Kumar, S. Thareja, J. Naik, J.P. Yadav, P. Pathak, M. Grishina, A. Verma, H. Khalilullah, M. Jaremko, A.-H. Emwas and P. Kumar, *Pharmaceuticals*, **16**, 299 (2023); https://doi.org/10.3390/ph16020299
8. B. Dubey, K. Singh, A. Kumar, S.P. Kushwaha and Suvaiv, *Biochem. Cell. Arch.*, **25**, 1301 (2025); https://doi.org/10.51470/BCA.2025.25.2.1301
9. R. Cheke, S. Firke, R. Patil and S. Bari, *Cent. Nerv. Syst. Agents Med. Chem.*, **18**, 76 (2018); https://doi.org/10.2174/1871524917666171113124112
10. A. Kale, R. Kakde, S. Pawar, R. Thombare, D. Zope and I. Kakde, *Curr. Drug Discov. Technol.*, **22**, e070524229730 (2025); https://doi.org/10.2174/0115701638299019240418055933
11. R.K. Kushwaha, K. Singh, S.P. Kushwaha, D. Chandra, A. Kumar and P. Kumar, *Ann. Phytomed.*, **11**, 385 (2022); https://doi.org/10.54085/ap.2022.11.2.46
12. R. Nath, M.S. Yar, S. Pathania, G. Grover, B. Debnath and M.J. Akhtar, *J. Mol. Struct.*, **1228**, 129742 (2021); https://doi.org/10.1016/j.molstruc.2020.129742
13. V.R. Solomon, C. Hu and H. Lee, *Bioorg. Med. Chem.*, **17**, 7585 (2009); https://doi.org/10.1016/j.bmc.2009.08.068
14. V. Abbot, P. Sharma, S.S. Dhiman, M.N. Noolvi, H. Patel and V. Bhardwaj, *RSC Adv.*, **7**, 28313 (2017); https://doi.org/10.1039/C6RA24662A
15. K. Liu, Y. Ding and C. Kang, *Pharm. Chem. J.*, **54**, 345 (2020); https://doi.org/10.1007/s11094-020-02215-w
16. A.M. Mokhtar, S.M. El-Messery, M.A. Ghaly and G.S. Hassan, *Bioorg. Chem.*, **104**, 104259 (2020); https://doi.org/10.1016/j.bioorg.2020.104259
17. P. Storici, D. De Biase, F. Bossa, S. Bruno, A. Mozzarelli, C. Peneff, R. Silverman and T. Schirmer, *J. Biol. Chem.*, **279**, 363 (2004); https://doi.org/10.1074/jbc.M305884200
18. S.J. Gilani, M.Z. Hassan, S.S. Imam, C. Kala and S.P. Dixit, *Bioorg. Med. Chem. Lett.*, **29**, 1825 (2019); https://doi.org/10.1016/j.bmcl.2019.05.007
19. D.J. Diller and K.M. Merz Jr., *Proteins*, **43**, 113 (2001); https://doi.org/10.1002/1097-0134(20010501)43:2<113::AID-PROT1023>3.0.CO;2-T
20. M.M. Castel-Branco, G.L. Alves, I.V. Figueiredo, A. Falcão and M.M. Caramona, *Methods Find. Exp. Clin. Pharmacol.*, **31**, 101 (2009); https://doi.org/10.1358/mf.2009.31.2.1338414
21. S. Sinha, K. Singh, A. Ved, K.S. Shukla, S. Mujeeb and M.K. Kashyap, *Afr. J. Biomed. Res.*, **27**, 4668 (2024); https://doi.org/10.53555/AJBR.v27i3S.3061
22. S.L. Khokra, K. Arora, S.A. Khan, P. Kaushik, R. Saini and A. Husain, *Iran. J. Pharm. Res.*, **18**, 1 (2019).
23. M. Castel-Branco, V. Lebre, A. Falcão, I. Figueiredo and M. Caramona, *Eur. J. Pharmacol.*, **482**, 163 (2003); https://doi.org/10.1016/j.ejphar.2003.09.065
24. S.M. Kamruzzaman, L. Bulbul, M.Z. Alam and M.M. Rahman, *Heliyon*, **9**, e18295 (2023); https://doi.org/10.1016/j.heliyon.2023.e18295
25. K. Lidster, J.G. Jefferys, I. Blümcke, V. Crunelli, P. Flecknell, B.G. Frenguelli, W.P. Gray, R. Kaminski, A. Pitkänen, I. Ragan, M. Shah, M. Simonato, A. Trevelyan, H. Volk, M. Walker, N. Yates and M. J. Prescott, *J. Neurosci. Methods*, **260**, 2 (2016); https://doi.org/10.1016/j.jneumeth.2015.09.007
26. A. Kumar, A.K. Shakya and K. Singh, *Ann. Phytomed.*, **11**, 373 (2022); https://doi.org/10.54085/ap.2022.11.2.44
27. J.R. Dimmock, S.C. Vashishtha and J.P. Stables, *Eur. J. Med. Chem.*, **35**, 241 (2000); https://doi.org/10.1016/S0223-5234(00)00123-9
28. N. Siddiqui and W. Ahsan, *Arch. Pharm.*, **342**, 462 (2009); https://doi.org/10.1002/ardp.200900002
29. N. Siddiqui, P. Ahuja, S. Malik and S.K. Arya, *Arch. Pharm.*, **346**, 819 (2013); https://doi.org/10.1002/ardp.201300083